Editors' Suggestion

Lieb-Robinson causality and non-Fermi liquids

Subham Dutta Chowdhury and Aditya Hebbar
The Abdus Salam ICTP, Strada Costiera 11, 34151 Trieste, Italy

Sean A. Hartnoll
DAMTP, University of Cambridge, Cambridge CB3 0WA, United Kingdom

(Received 3 December 2025; accepted 18 May 2026; published 12 June 2026)

Quantum mechanical lattice models with local, bounded interactions obey Lieb-Robinson causality. We show that this implies a domain of analyticity of the retarded Green's function $G^R(\omega, \mathbf{k})$ of local lattice operators as a function of complex frequency ω and momentum $\mathbf{k}$, similar to the light-cone analyticity property of relativistic field theories. Low-energy effective descriptions of the dynamics must be consistent with this microscopic analyticity constraint. We consider two canonical low-energy fermionic Green's functions describing non-Fermi liquids, the marginal Fermi liquid and the "Hertz liquid." The pole in these Green's functions must be outside of the Lieb-Robinson domain of analyticity for all complex momenta captured by the low-energy theory. This constraint upper bounds the magnitude of the dimensionless non-Fermi-liquid coupling in certain Hertz liquids.

DOI: 10.1103/1q5b-3w57

I. INTRODUCTION

Light-cone causality is a foundational principle in relativistic quantum field theory. Local operators commute at spacelike separation, leading to analyticity properties of the S-matrix and, through the Källén-Lehmann representation, retarded Green's functions. Analyticity connects high- and low-energy dynamics, enabling bootstrap approaches to quantum fields [1–3], including in cases where Lorentz invariance is broken by temperature, charge density, or magnetic field [4–10].

The Lieb-Robinson bound extends the notion of a light cone to local lattice models with bounded interactions [11]. As a localized operator evolves in time through repeated commutation with a local lattice Hamiltonian, each commutation can only cause the operator to spread in space by a finite amount. The spatial growth of the operator is thereby bounded by the amount of time that has passed. A rigorous treatment of this effect—we will follow Refs. [12,13]—shows that the time-evolved operator has an exponentially small norm outside of a light cone defined by the Lieb-Robinson velocity. The Lieb-Robinson velocity v is, up to numerical factors, the lattice spacing multiplied by the norm of the local terms in the Hamiltonian—see (3) below. It was argued in Ref. [14] that Lieb-Robinson causality could be used, in an analogous way to relativistic causality, to bound low-energy observables.

Here, we obtain sharp causality bounds on low-energy observables arising from lattice models. In (7) and in Fig. 1 below we establish a domain of analyticity of retarded Green's functions, as a function of frequency ω and momentum $\mathbf{k}$, in lattice models that are subject to a Lieb-Robinson bound. The domain restricts the imaginary parts of the frequency and momentum—see (4) below. At low frequencies and momenta the domain of analyticity is the same as that obtained for relativistic theories, with v the effective speed of light.

Non-Fermi liquids are ubiquitous in strongly correlated materials, exhibiting unconventional transport and thermodynamic properties [15,16]. They present a major theoretical challenge due to strong interactions between the electrons [17–19]. These interactions can be probed using angle-resolved photoemission spectroscopy (ARPES) [20,21], that measures the electronic retarded Green's function $G^R(\omega, \mathbf{k})$. We will show that analyticity properties of $G^R(\omega, \mathbf{k})$, following from Lieb-Robinson causality, constrain the space of possible non-Fermi-liquid theories that can emerge at low frequencies.

Any pole in the electronic Green's function $G^R(\omega, \mathbf{k})$ must remain outside of the Lieb-Robinson domain of analyticity. We will review below some canonical non-Fermi-liquid Green's functions, including the marginal Fermi liquid and a phenomenological generalisation of Hertz theory. These models are assumed to pertain below some cutoff energy Λ. The parameters in the models are then the "quasiparticle residue" $\mathcal{A}$, a dimensionless coupling λ, and a renormalized Fermi velocity $v_F^\star$. Clearly one expects $v_F^\star < v$. In (16) we further establish an upper bound on the coupling $|\lambda|$ in cases where the fermionic excitation remains well defined at the lowest-energy scales but has a non-Fermi-liquid decay rate [i.e., $\omega < |\mathrm{Im}\,\Sigma(\omega)| < \omega^2$ as $\omega \to 0$]. Our bound is consistent with ARPES data in overdoped cuprates, as fit in Refs. [22,23]. In cases with stronger departures from Fermi-liquid theory at low energies all velocities are driven to zero and there is no bound on λ from causality.

Published by the American Physical Society under the terms of the Creative Commons Attribution 4.0 International license. Further distribution of this work must maintain attribution to the author(s) and the published article's title, journal citation, and DOI.

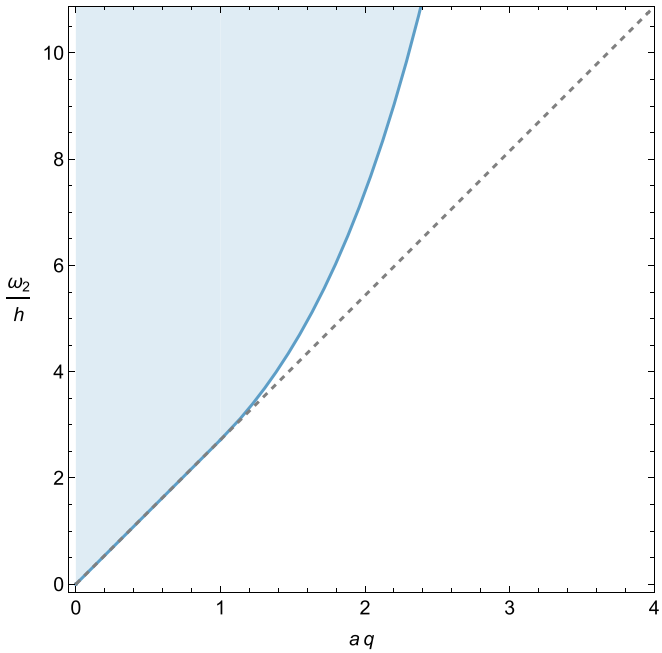


FIG. 1. The retarded Green's function must be analytic in the shaded region, given by (7). The dashed line shows the Lieb-Robinson light cone with the velocity defined in (3).

We proceed to obtain the bound (19) on the magnitude $|G^R(\omega, \mathbf{k})|$ of the Green's function within the domain of analyticity. This bound implies the upper bound (20) on the quasiparticle residue $\mathcal{A}$. Finally, in the discussion section we extend our framework to the retarded Green's function for the current operator. Within the Drude model of transport, our upper bound on $|G^R(\omega, 0)|$ leads to an upper bound on the dc conductivity.

II. ANALYTICITY FROM LIEB-ROBINSON CAUSALITY

Let the operator $\psi_\alpha^\dagger$ create a fermion at the site α of a lattice, which is at position $\mathbf{x}_\alpha$. We have suppressed any fermion spin label. The fermionic retarded Green's function is

$$G^R(\omega, \mathbf{k}) \equiv -i \sum_\alpha \int_0^\infty dt\, e^{i\omega t - i\mathbf{k}\cdot\mathbf{x}_\alpha} \langle \{\psi_\alpha^\dagger(t), \psi_0(0)\}\rangle. \quad (1)$$

Here, $\langle\cdot\rangle \equiv \frac{1}{\mathcal{Z}}\mathrm{tr}(\cdot\, e^{-H/T})$, with $\mathcal{Z} \equiv \mathrm{tr}\, e^{-H/T}$ the partition function. A domain of analyticity of $G^R(\omega, \mathbf{k})$ will follow from controlling the integral (1) for complex $(\omega, \mathbf{k})$. The correlation function is bounded by the operator norm $|\langle\{\psi_\alpha^\dagger(t), \psi_0(0)\}\rangle| \leqslant \|\{\psi_\alpha^\dagger(t), \psi_0(0)\}\| \equiv C(t, \mathbf{x}_\alpha)$. Lieb-Robinson (see Appendix A) is the further bound,

$$C(t, \mathbf{x}) < \begin{cases} K\left(\frac{eht}{x/a}\right)^{x/a} & \text{for } x/a > eht, \\ 2 & \text{for } x/a < eht. \end{cases} \quad (2)$$

Here, for simplicity, we have restricted to a square lattice in d spatial dimensions with lattice spacing a and with a translationally invariant nearest-neighbour Hamiltonian given by an operator H on each edge. These assumptions are not essential. In (2) we set $x \equiv |\mathbf{x}|$, $h \equiv 4(2d-1)||H||$, and $K \equiv \frac{2d}{2d-1}$. That is, h is the largest energy scale of a local term in the Hamiltonian. We see in (2) that $C(t, \mathbf{x})$ is forced to decay exponentially outside the "light cone" $x = vt$, where the Lieb-Robinson velocity

$$v \equiv eha. \quad (3)$$

Denote the imaginary parts

$$\omega_2 \equiv \mathrm{Im}\,\omega, \quad \mathbf{q} \equiv \mathrm{Im}\,\mathbf{k}. \quad (4)$$

While not as familiar in many-body theory as complex energies, complex momenta are a standard ingredient of bootstrap analyticity arguments (see, e.g., Refs. [1–7,9] for recent uses similar in spirit to ours). The imaginary part $\mathbf{q}$ is not restricted to the Brillouin zone. Convergence of the Fourier transform in (1) depends on the competition between the nonoscillatory exponential terms from the imaginary parts (4) and the exponential decay in (2). Consider the absolute value

$$|G^R(\omega, \mathbf{k})| \leqslant \sum_\alpha \int_0^\infty dt\, e^{-\omega_2 t + q x_\alpha} C(t, \mathbf{x}_\alpha). \quad (5)$$

Here, we set $q = |\mathbf{q}|$ and $x_\alpha = |\mathbf{x}_\alpha|$ and used $\mathbf{q}\cdot\mathbf{x}_\alpha \leqslant q x_\alpha$. The convergence of (5) is determined by the behavior of the integrand at large t and x_α. In this regime we may think of $x_\alpha \to x$, a continuous variable. Consider then the Fourier transform along the line $t = \gamma\frac{x}{a}$, and look at the behavior at large x/a and fixed γ. Using (2) the integrand in (5) is bounded by

$$\begin{cases} K\, e^{-[\omega_2\gamma - aq - \log(eh\gamma)]\frac{x}{a}} & \text{if } eh\gamma \leqslant 1, \\ 2\, e^{-[\omega_2\gamma - aq]\frac{x}{a}} & \text{if } eh\gamma \geqslant 1. \end{cases} \quad (6)$$

For the integral to converge we need the exponents in (6) to be negative for all γ. Depending on ω_2, either the first or the second line in (6) will impose the stronger constraint. In the first line, the minimum of the quantity in square brackets in the exponent is reached at $\gamma = 1/\omega_2$. Requiring the exponent to be negative at this value gives the constraint $\omega_2 > he^{aq}$. This will be the strongest constraint on ω_2 and q when the minimum is within the domain of applicability of the first line, $eh\gamma \leqslant 1$. That is, this is the strongest constraint for $\omega_2 \geqslant eh$. If instead $\omega_2 \leqslant eh$ then the strongest constraint occurs at the boundary $eh\gamma = 1$. A negative exponent at this value requires $\omega_2 > ehaq$. Putting the above results together we find that the integral converges for

$$\begin{cases} \omega_2 > he^{aq} & \text{for } \omega_2 \geqslant eh, \\ \omega_2 > ehaq & \text{for } \omega_2 \leqslant eh. \end{cases} \quad (7)$$

The retarded Green's function $G^R(\omega, \mathbf{k})$ is analytic in the domain of convergence (7). Analyticity holds because differentiating with respect to ω or $\mathbf{k}$ brings down factors of t or x inside the integral that are subleading compared to the exponential suppression (6) in the domain of convergence. The real parts of the frequency and momentum are unconstrained. Figure 1 shows a plot of the region (7). At low frequencies the bound defines a light cone with the Lieb-Robinson velocity v in (3). At frequencies above the microscopic energy eh the bound (7) becomes weaker and does not efficiently enforce analyticity at imaginary momenta well above the inverse lattice spacing.

III. LOW-ENERGY DYNAMICS CLOSE TO A FERMI SURFACE

The Fermi surface is the singular locus of the Green's function at zero energy. Momenta on the Fermi sufrace obey $G^R(0, \mathbf{k}_F) = \infty$ [24,25]. To focus on low-energy excitations we set $\mathbf{k} = \mathbf{k}_F + \mathbf{k}_\perp$, where $\mathbf{k}_\perp$ is orthogonal to the Fermi surface. The effective theories we are about to describe arise by expanding the full Green's function at small ω and $k_\perp \equiv |\mathbf{k}_\perp|$. These theories hold only at low frequencies and momenta, below cutoffs Λ and $\bar{\Lambda}$,

$$|\omega| \ll \Lambda \quad \text{and} \quad k_\perp \ll \bar{\Lambda}. \tag{8}$$

The *marginal Fermi liquid* (MFL) was originally proposed as a phenomenological model for the normal state of the cuprate high-temperature superconductors [26,27]. The low-energy Green's function is

$$G^R_{\rm MFL}(z, \mathbf{k}) = \frac{\mathcal{A}}{z - v_F^\star k_\perp - \Sigma_{\rm MFL}(z)}. \tag{9}$$

Here, $v_F^\star$ is the renormalized Fermi velocity and we have used z to emphasize that we are interested in complex frequencies. The self-energy takes the form

$$\Sigma_{\rm MFL}(z) = \lambda\, z \log\left(\frac{-iz}{\Lambda}\right) + O\left(\frac{z^2}{\Lambda}\right), \tag{10}$$

where $\lambda \geqslant 0$ is the coupling and Λ is the cutoff energy scale (8). In (10) any additional linear-in-z terms in the self-energy have been absorbed into a rescaling of the bare z term, leading to the nontrivial weight $\mathcal{A} \neq 1$ in the numerator of (9). Higher-order analytic corrections to the self-energy must be retained in (10) but, as indicated, are suppressed relative to the bare term by powers of z/Λ. We will drop these terms in the remainder. We will remain at a fixed $\mathbf{k}_F$. The only singular $k_\perp$ dependence in (9) is in the dispersion about the Fermi surface.

A *Hertz liquid* arises from scattering of fermions by a critical boson [28,29]. We will view the Hertz liquid as a phenomenological low-energy model that generalizes the MFL to a continuous exponent α (cf. Refs. [22,23,30]),

$$G^R_{\rm Hertz}(z, \mathbf{k}) = \frac{\mathcal{A}}{z - v_F^\star k_\perp - \Sigma_{\rm Hertz}(z)}, \tag{11}$$

now with

$$\Sigma_{\rm Hertz}(z) = -i\lambda \frac{(-iz)^\alpha}{\Lambda^{\alpha-1}} + O\left(\frac{z^2}{\Lambda}\right). \tag{12}$$

The factors of Λ define λ as the dimensionless coupling at the cutoff scale. A MFL arises in the limit $\alpha \to 1$ (with Λ fixed take $\mathcal{A} \approx \frac{\alpha-1}{\lambda_{\rm MFL}}\mathcal{A}_{\rm MFL}$, $v_F^\star \approx \frac{\alpha-1}{\lambda_{\rm MFL}} v_{F\,\rm MFL}^\star$, and $\lambda \approx -1 + \frac{\alpha-1}{\lambda_{\rm MFL}}$) whereas $\alpha = 2$ is a conventional Fermi liquid. In general, α can take any positive value. For $\alpha < 2$ the leading low-energy behavior of the self-energy is non-Fermi liquid. At real frequencies ω we have

$$\mathrm{Im}\,\Sigma_{\rm Hertz}(\omega) = -\lambda \cos\left(\frac{\alpha\pi}{2}\right) \frac{|\omega|^\alpha}{\Lambda^{\alpha-1}}. \tag{13}$$

The requirement that $\mathrm{Im}\,\Sigma < 0$ fixes the sign of λ. For $\alpha \in (0, 1)$ we have $\lambda > 0$ while for $\alpha \in (1, 3)$ we must have $\lambda = -|\lambda| < 0$.

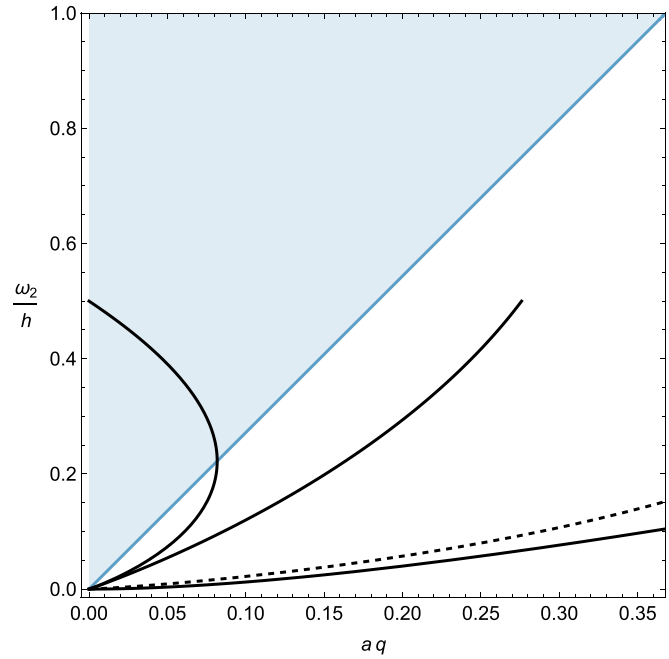


FIG. 2. Motion of the pole (14) over $0 \leqslant \omega_2 \leqslant \Lambda$, with $\Lambda = \frac{1}{2}h$, $v_F^\star = \frac{1}{3}v$. The Dashed line is a $\lambda = 1$ MFL. Solid black lines are Hertz liquids with (top to bottom) $\{\alpha = \frac{3}{2}, \lambda = -1\}$, $\{\alpha = \frac{3}{2}, \lambda = -\frac{1}{2}\}$, and $\{\alpha = \frac{1}{2}, \lambda = 1\}$. The top curve enters the shaded region, excluded by the causality bound (7).

IV. CAUSALITY BOUNDS

The pole in the retarded Green's functions (9) and (11), which are valid at low momenta and energies (8), must remain outside of the domain of analyticity (7). We will probe this constraint along the imaginary momenta $k_\perp = iq$. The self-energies (10) and (12) are purely imaginary when $z = i\omega_2$, with $\omega_2 > 0$. We can write $\Sigma(i\omega_2) \equiv i\sigma(\omega_2)$, i.e., $\sigma_{\rm MFL}(\omega_2) = \lambda\, \omega_2 \log \frac{\omega_2}{\Lambda}$ and $\sigma_{\rm Hertz}(\omega_2) = -\lambda\, \omega_2^\alpha / \Lambda^{\alpha-1}$, and the pole is at

$$v_F^\star q = \omega_2 - \sigma(\omega_2). \tag{14}$$

Consider first a Hertz liquid with $1 < \alpha < 3$. These are mild non-Fermi liquids, as the nonanalytic self-energy is subleading at low frequencies compared to the bare ω term in (11) and (14). As $\omega \to 0$ the condition for the pole to be outside the analytic region (7) is

$$v_F^\star < v. \tag{15}$$

The bare Fermi velocity is always below the Lieb-Robinson velocity [13], and interactions tend to renormalize the Fermi velocity down. Hence (15) is a reasonable expectation, now proven for this Hertz liquid.

Now assume that (15) holds. As the frequency is increased the location of the pole (14) starts to move towards the region of analyticity, recalling that $\lambda = -|\lambda|$ is negative for $1 < \alpha < 3$. The motion of the pole is illustrated in Fig. 2. To see how far the pole gets we can evaluate its location at the cutoff $\omega_2 = \Lambda$. From (14) the cutoff is reached at momentum q_Λ given by $v_F^\star q_\Lambda = \Lambda(1 - |\lambda|)$. For the theory to be consistent with causality, the point (q_Λ, Λ) must be outside of the analytic region (7). Typically the cutoff $\Lambda \lesssim h$, the microscopic

energy scale. This (inessential) assumption simplifies the condition for causality in (7) to $\Lambda < v q_\Lambda$. Thus we must have

$$|\lambda| < 1 - \frac{v_F^\star}{v} \qquad (\text{for } 1 < \alpha < 3). \tag{16}$$

In (16) we have obtained a rigorous upper bound on the dimensionless coupling constant of a Hertz liquid. Figure 2 shows two instances of Hertz liquids with $1 < \alpha < 3$, one that respects the bound (16) and one which does not. The bound (16) resembles bounds in Ref. [9] established for relativistic fluids and superfluids.

Now consider the MFL and Hertz liquid with $\alpha < 1$. The self-energy is strongly singular at low frequencies and dominates the dispersion of the pole in (14). As $\omega \to 0$ the pole is well outside the analytic region (see Fig. 2), and there is no constraint on $v_F^\star$ [31]. If (15) holds, then

$$\omega_2 < \omega_2 - \sigma(\omega_2) = v_F^\star q < v q \quad (\text{MFL or } \alpha < 1). \tag{17}$$

The first inequality here follows for the MFL from the fact that the log is negative for $\omega_2 < \Lambda$ and for the $\alpha < 1$ Hertz liquid from the fact that λ is positive. The bound (17) implies that the pole is outside of the region of analyticity in these models, for all values of the coupling. As a consistency check we can verify that the coupling bound (16) is automatically obeyed in the $\alpha \to 1$ limit of a Hertz liquid described below (12), leading to a MFL.

To intuitively understand the absence of a coupling bound in the strongly singular cases, define a group velocity $v_g(\omega) \equiv d\omega/dk_\perp = v_F^\star/[1 - \partial_\omega \operatorname{Re}\Sigma(\omega)]$. When the self-energy dominates at low energies, $\partial_\omega \operatorname{Re}\Sigma(\omega) \to -\infty$ and the group velocity goes to zero. That is to say, low-energy excitations move increasingly slowly and this is why there is no constraint from causality in these cases.

A Hertz liquid has been used to fit ARPES data in cuprates, with the exponent α evolving as a function of doping [22,23]. The data were fit to a more complicated temperature-dependent self-energy that reduces to (11) at zero temperature. For the overdoped samples it was found that $1 < \alpha < 2$ with a coupling $\bar{\lambda} \approx 0.5$ that is roughly independent of α. It is not straightforward to convert $\bar{\lambda}$ to our bounded coupling λ [32]. However, the measured $\bar{\lambda}$ remains constant through the MFL value of $\alpha = 1$. As explained above, a Hertz liquid that continuously crosses over to a MFL is automatically causal. In this sense, the data are consistent with our bound.

V. BOUND ON THE QUASIPARTICLE RESIDUE

Performing the integral in (5) gives an explicit upper bound on the Green's function within the domain of analyticity. The integrand in (5) is split, using (6), into parts inside and outside of the light cone $x_\alpha = vt$. We will focus on imaginary frequencies $\omega_2 < eh$—any low-energy effective description will be within this regime. For these frequencies, as explained below (6), the integrand is maximised on the light cone. Thus we obtain

$$\begin{aligned} |G^R(\omega, \mathbf{k})| &< \sum_\alpha \left[K \int_0^{\frac{x_\alpha}{v}} dt\, e^{-\frac{\omega_2 x_\alpha}{v}} + 2 \int_{\frac{x_\alpha}{v}}^\infty dt\, e^{-\omega_2 t} \right] e^{q x_\alpha} \\ &= \sum_\alpha \left[\frac{K}{v} x_\alpha + \frac{2}{\omega_2} \right] e^{-(\frac{\omega_2}{v} - q) x_\alpha}. \end{aligned} \tag{18}$$

Noting that $K \leqslant 2$ and $\frac{1}{\omega_2} \leqslant \frac{1}{\omega_2 - vq}$, then from (18)

$$\begin{aligned} |G^R(\omega, \mathbf{k})| &< \sum_\alpha \left[\left(\frac{\omega_2}{v} - q \right) x_\alpha + 1 \right] \frac{2 e^{-(\frac{\omega_2}{v} - q) x_\alpha}}{\omega_2 - vq} \\ &\leqslant \frac{2 c_d (eh)^d}{(\omega_2 - vq)^{d+1}}. \end{aligned} \tag{19}$$

We have verified the second step numerically, using $0 < \frac{\omega_2}{eh} - aq \leqslant \frac{\omega_2}{eh} < 1$. In (19), $c_d = \sum_{\vec{n} \in \mathbb{Z}^d} (|\vec{n}| + 1) e^{-|\vec{n}|} \approx \{4.005, 18.86, 100.6\}$ for $d = 1, 2, 3$, respectively.

Using the Green's functions (9) and (11) in the bound (19), and setting $q = 0$, one finds that the right-hand side of (19) decreases with frequency while the left-hand side increases. The strongest constraint is therefore from the upper limit $\omega_2 = \Lambda < eh$, giving

$$\mathcal{A} \leqslant 2\, c_d \left(1 - \frac{\sigma(\Lambda)}{\Lambda} \right) \left(\frac{eh}{\Lambda} \right)^d. \tag{20}$$

Recall that $\sigma(\omega_2)$ was introduced above (14). It is notable that (20) is obtained purely from causality considerations. For the MFL and Hertz liquid with $\alpha < 1$ this bound on $\mathcal{A}$ is weaker than the general expectation that $\mathcal{A} \leqslant 1$. For a Hertz liquid with $\alpha > 1$ the bound can be a nontrivial constraint. If the pole is close to the analytic region, then $1 - \frac{\sigma(\Lambda)}{\Lambda} \approx v_F^\star / v$. Whenever there is strong mass renormalization or when the Fermi momentum is small compared to lattice scales, then $v_F^\star / v \ll 1$ and the right-hand side of (20) becomes small.

The bounded Green's functions are those measured by ARPES, involving the microscopic lattice fermion creation operator, as opposed to some renormalized operator defined within an effective field theory. With this in mind, a featureless "incoherent" spectral weight should be added to the low-energy Green's functions. The incoherent contribution does not affect our previous analyticity arguments, but will shift the absolute value of the Green's function. Our bound (20) assumes that the incoherent contribution is small compared to the non-Fermi-liquid peaks (9) and (11).

VI. DISCUSSION

We have shown that Lieb-Robinson causality implies a domain of analyticity (7) and an upper bound (19) on the Green's function within that domain. We have used these facts to bound the coupling constant and quasiparticle residue of certain non-Fermi liquids.

The mathematical handle on lattice causality that we have developed here is a key step in building a quantum lattice bootstrap program of the kind envisioned in Ref. [33], in analogy with endeavors such as the S-matrix [34–36] or conformal [37–39] bootstraps. An important question for future work is whether there is a bootstrap bound on the coupling constant for the case of a marginal Fermi liquid. A heuristic

argument for a such a bound was given in Ref. [17] and, as noted there, it would imply a Planckian bound for an important class of strange metallic systems.

Our Lieb-Robinson causality constraints also apply to the Green's functions of conserved densities and currents, leading to bounds on transport. A light-cone bound on the diffusivity was proposed in Ref. [14], and made sharp for relativistic causality in Refs. [5,6] and for open lattice systems in Ref. [40]. The analyticity properties that we have established in the present paper mean that the bounds in Refs. [5,6] extend to diffusion in local lattice systems (as we noted preemptively in Ref. [33]). In Appendix B we show, furthermore, that the upper bound (19) translates into an upper bound on the conductivity whenever low-energy transport is described by the Drude model [41].

ACKNOWLEDGMENTS

This work has been partially supported by STFC consolidated Grant No. ST/T000694/1. S.A.H. is partially supported by Simons Investigator award No. 620869. S.D.C. and A.H. are supported by "Exotic High Energy Phenomenology" (X-HEP), a project funded by the European Union Grant Agreement No. 101039756 (PI: J. Elias Miró). Views and opinions expressed are however those of the author(s) only and do not necessarily reflect those of the European Union or the ERC Executive Agency (ERCEA). Neither the European Union nor the granting authority can be held responsible for them.

DATA AVAILABILITY

There are no publicly available research data or software supporting this manuscript. Requests for further information or data should be sent to the authors.

APPENDIX A: LIEB-ROBINSON BOUND

This Appendix outlines a proof of the Lieb-Robinson bound, roughly following Refs. [12,13]. This will lead to (2) in the main text. In order to obtain explicit expressions, we consider a Hamiltonian on a d-dimensional square lattice, with nearest-neighbor interactions all given by the same local Hamiltonian H. More complicated lattices or longer-range interactions will only change the numerical value of the Lieb-Robinson velocity v. The local terms in the Hamiltonian can be thought of as living on the edges of the lattice, connecting pairs of vertices. If we wish to keep track of the edge ε in question, we will write H_ε. In addition to the operator norm $C(t, \mathbf{x}_\alpha)$, introduced in the main text, we will need to introduce the quantity

$$C_\varepsilon(t) \equiv \frac{||[H_\varepsilon(t), \psi_0(0)]||}{||H||}. \tag{A1}$$

The time dependence here is generated using the full Hamiltonian $H_{\text{full}} = \sum_\varepsilon H_\varepsilon$, while H_ε is the local Hamiltonian on a single edge. Note that $||H_\varepsilon|| = ||H||$.

From the definition (A1) a sequence of deceptively simple manipulations [12,13] imply that

$$C(t, \mathbf{x}_\alpha) \leqslant C(0, \mathbf{x}_\alpha) + 2||H|| \sum_{\mathbf{x}_\alpha \in \varepsilon} \int_0^t C_\varepsilon(s) ds, \tag{A2}$$

where the sum is over all edges containing the vertex $\mathbf{x}_\alpha$. Furthermore, one has that

$$C_\varepsilon(t) \leqslant C_\varepsilon(0) + 2||H|| \sum_{\varepsilon' \cap \varepsilon, \varepsilon \neq \varepsilon'} \int_0^t C_{\varepsilon'}(s) ds. \tag{A3}$$

Here, the sum is over all edges ε' that share a vertex with ε, but do not coincide with ε. This final exclusion arises in the derivation of (A3) from the commutator $[H_{\text{full}}, H_\varepsilon] = \sum_{\varepsilon' \cap \varepsilon, \varepsilon \neq \varepsilon'} [H_{\varepsilon'}, H_\varepsilon]$. The use of the two separate inequalities (A2) and (A3) accounts for the fact that $C(t, \mathbf{x}_\alpha)$ involves an anticommutator while $C_\varepsilon(t)$ involves a commutator. This separation also allows us to avoid taking a supremum over operators that is commonly used in derivations of the bound.

We can iterate (A3) by using the left-hand side in the integral on the right-hand side. This produces a sequence of edges $\varepsilon, \varepsilon_1, \varepsilon_2, \ldots$. For each iteration, the first term on the right-hand side of (A3) is zero unless the edge ε_k is adjacent to the origin. Let $r \equiv D(\mathbf{x}_\alpha)$ be the Manhattan norm of $\mathbf{x}_\alpha$. This is the minimal number of edges that must be traversed to get from the origin to $\mathbf{x}_\alpha$. A given sequence of edges $\varepsilon, \varepsilon_1, \varepsilon_2, \ldots$ defines path in the lattice. It follows that $C_{\varepsilon_k}(0) = 0$ in (A3) for $k < r - 1$. Thus, by iterating we obtain the bound

$$\begin{aligned} C_\varepsilon(t) &\leqslant (2||H||)^{r-1} \\ &\quad \times \sum_{\varepsilon_1 \cdots \varepsilon_{r-1}} \int_0^t ds_1 \cdots \int_0^{s_{r-2}} ds_{r-1} C_{\varepsilon_{r-1}}(s_{r-1}) \\ &\leqslant 2 \frac{(4(2d-1)t||H||)^{r-1}}{(r-1)!}. \end{aligned} \tag{A4}$$

The second line uses the bound $C_{\varepsilon_{r-1}}(s_{r-1}) \leqslant 2$ and the fact that, given an edge ε on a square lattice, there are $2(2d-1)$ edges ε' obeying the conditions in the sum (A3).

Using (A4) in (A2) gives

$$C(t, \mathbf{x}_\alpha) \leqslant K \frac{(ht)^r}{r!}. \tag{A5}$$

Here, we introduced

$$h \equiv 4(2d-1)||H||, \quad K \equiv \frac{2d}{2d-1}, \tag{A6}$$

and used the fact that there are $2d$ edges connecting to the vertex $\mathbf{x}_\alpha$. The first term in (A2) is zero unless $\mathbf{x}_\alpha$ coincides with the origin. Thus (A5) holds for all $r \geqslant 1$. Now, for a fermion creation operator $\|\psi_0^\dagger(0)\psi_0(0)\| = 1$ and hence we always have $C(t, \mathbf{x}) \leqslant 2$, with the factor of 2 from the anticommutator. This allows us to strengthen the bound (A5) to

$$\begin{aligned} C(t, \mathbf{x}_\alpha) &\leqslant \min\left(2, K \frac{(ht)^{D(\mathbf{x}_\alpha)}}{D(\mathbf{x}_\alpha)!}\right) \\ &< \min\left[2, K\left(\frac{eht}{D(\mathbf{x}_\alpha)}\right)^{D(\mathbf{x}_\alpha)}\right]. \end{aligned} \tag{A7}$$

Here, we reintroduced the Manhattan norm explicitly, setting $r \equiv D(\mathbf{x}_\alpha)$. The second inequality in (A7) uses a standard bound on the factorial.

For the arguments in the main text to go through we will want to use the final expression in (A7) as the upper bound for $x/a > eht$, and the upper bound of 2 for $x/a < eht$. This restriction allows us to get rid of the Manhattan norm in (A7). The Manhattan norm is necessarily greater than the Euclidean norm, $D(\mathbf{x}) \geqslant x/a$ with $x = |\mathbf{x}|$, and furthermore the function $f(x) = (ex_o/x)^x$ is monotonically decreasing for $x > x_o$. That is, we can replace $D(\mathbf{x})$ by x/a in the final expression in (A7) whenever $x/a > ht$. This is a weaker condition than our requirement that $x/a > eht$. That is, we can take

$$C(t,\mathbf{x}) < \begin{cases} K\left(\frac{eht}{x/a}\right)^{x/a} & \text{for } x/a > eht, \\ 2 & \text{for } x/a < eht, \end{cases} \tag{A8}$$

which is (2) in the main text.

APPENDIX B: CONDUCTIVITY BOUND

The conductivity is closely related to the diffusivity but is a distinct concept. Indeed, we will be able to set $\mathbf{k} = \mathbf{0}$ to obtain a conductivity bound and hence the only assumption for the low-energy description is that the optical response is given by the Drude model [41]. That is to say, the Green's function for the current density operator j at $\mathbf{k} = \mathbf{0}$ takes the form

$$G^R_{jj}(\omega) = \frac{i\omega\sigma_o}{1 - i\omega\tau}. \tag{B1}$$

Here, σ_o is the dc conductivity and τ is the current relaxation lifetime.

In order to apply the bound (19) to the Green's function (B1) we must first reintroduce the norm $||\mathcal{O}||$ of the local lattice operator whose Green's function is being bounded. The fermionic Green's functions in the main text had $||\psi_0|| = 1$. Thus (19) is more generally written

$$\left|G^R_{OO}(\omega,\mathbf{k})\right| < \frac{2c_d(eh)^d||\mathcal{O}||^2}{(\omega_2 - vq)^{d+1}}. \tag{B2}$$

Setting $\omega = i\omega_2$, $\mathbf{k} = \mathbf{0}$, and using (B1) in (B2) gives an upper bound on the dc conductivity,

$$\sigma_o \leqslant \frac{2\,c_d||j_0||^2}{a^d}\frac{1+\omega_2\tau}{\omega_2^2}\left(\frac{eh}{\omega_2}\right)^d. \tag{B3}$$

The factor of a^d appears due to converting the density operator j into the on-site operator j_0 (see the recent discussion in Ref. [33]). The right-hand side of (B3) is a decreasing function of ω_2 and hence the strongest bound is obtained at large $\omega_2 = \Lambda < eh$. Here, Λ is the cutoff frequency for the validity of the Drude model.

To get a sense for the consequences of (B3), we can estimate $||j_0|| \sim ah$ and suppose that the Drude peak extends up to a finite fraction of the microscopic scale, so that $\Lambda \sim h$. Furthermore, the Drude model requires $1 \lesssim h\tau$ in order for the relaxation time to be within the regime of validity of the model. Then, up to numerical factors, we would have from (B3) that

$$\sigma_o \lesssim a^{2-d}h\tau. \tag{B4}$$

The usual Drude formula for conduction by well-defined quasiparticles is $\sigma_o \sim k_F^{d-2}E_F\tau$. Here $E_F \sim k_F v_F$ is the Fermi energy. For a large Fermi surface with $k_F \sim \pi/a$ we see that (B4) becomes $v_F \lesssim v$. This is reassuringly consistent. It should be emphasized, however, that from a low-energy perspective the two parameters σ_o and τ in (B1) are logically independent. The causality bound (B4) can then be read as stating that, regardless of the microscopic mechanism for charge transport, the conductivity cannot be parametrically larger than the value expected from classical Drude theory. Essentially the same conclusion is reached from the causality upper bound on diffusivity [14], demonstrating a consistency between the various facets of Lieb-Robinson causality.

[1] M. Correia, A. Sever, and A. Zhiboedov, An analytical toolkit for the S-matrix bootstrap, J. High Energy Phys. 03 (2021) 013.

[2] C. de Rham, S. Kundu, M. Reece, A. J. Tolley, and S.-Y. Zhou, Snowmass white paper: UV constraints on IR physics, arXiv:2203.06805.

[3] M. Kruczenski, J. Penedones, and B. C. van Rees, Snowmass white paper: S-matrix bootstrap, arXiv:2203.02421.

[4] P. Creminelli, O. Janssen, and L. Senatore, Positivity bounds on effective field theories with spontaneously broken Lorentz invariance, J. High Energy Phys. 09 (2022) 201.

[5] M. P. Heller, A. Serantes, M. Spaliński, and B. Withers, Rigorous bounds on transport from causality, Phys. Rev. Lett. **130**, 261601 (2023).

[6] M. P. Heller, A. Serantes, M. Spaliński, and B. Withers, The space of transport coefficients allowed by causality, Nat. Phys. **20**, 1948 (2024).

[7] P. Creminelli, O. Janssen, B. Salehian, and L. Senatore, Positivity bounds on electromagnetic properties of media, J. High Energy Phys. 08 (2024) 066.

[8] L. V. Delacrétaz, S. D. Chowdhury, and U. Mehta, Symmetry and causality constraints on Fermi liquids, J. High Energ. Phys. 10 (2025) 171.

[9] L. Hui, A. Nicolis, A. Podo, and S. Zhou, Microcausality without Lorentz invariance, J. High Energy Phys. 07 (2025) 188.

[10] C. P. Herzog, W. H. Pannell, B. Sahoo, and A. Stergiou, Magnetised bounds for conformal field theories, J. High Energ. Phys. **2026**, 121 (2026).

[11] E. H. Lieb and D. W. Robinson, The finite group velocity of quantum spin systems, Commun. Math. Phys. **28**, 251 (1972).

[12] M. B. Hastings, Locality in quantum systems, arXiv:1008.5137.

[13] C.-F. (Anthony) Chen, A. Lucas, and C. Yin, Speed limits and locality in many-body quantum dynamics, Rep. Prog. Phys. **86**, 116001 (2023).

[14] T. Hartman, S. A. Hartnoll, and R. Mahajan, Upper bound on diffusivity, Phys. Rev. Lett. **119**, 141601 (2017).

[15] A. J. Schofield, Non-Fermi liquids, Contemp. Phys. **40**, 95 (1999).

[16] G. R. Stewart, Non-Fermi-liquid behavior in d- and f-electron metals, Rev. Mod. Phys. **73**, 797 (2001).

[17] S. A. Hartnoll and A. P. Mackenzie, *Colloquium:* Planckian dissipation in metals, Rev. Mod. Phys. **94**, 041002 (2022).
[18] P. W. Phillips, N. E. Hussey, and P. Abbamonte, Stranger than metals, Science **377**, eabh4273 (2022).
[19] D. Chowdhury, A. Georges, O. Parcollet, and S. Sachdev, Sachdev-Ye-Kitaev models and beyond: Window into non-Fermi liquids, Rev. Mod. Phys. **94**, 035004 (2022).
[20] A. Damascelli, Z. Hussain, and Z.-X. Shen, Angle-resolved photoemission studies of the cuprate superconductors, Rev. Mod. Phys. **75**, 473 (2003).
[21] J. A. Sobota, Y. He, and Z.-X. Shen, Angle-resolved photoemission studies of quantum materials, Rev. Mod. Phys. **93**, 025006 (2021).
[22] T. J. Reber, X. Zhou, N. C. Plumb, S. Parham, J. A. Waugh, Y. Cao, Z. Sun, H. Li, Q. Wang, J. S. Wen, Z. J. Xu, G. Gu, Y. Yoshida, H. Eisaki, G. B. Arnold, and D. S. Dessau, A unified form of low-energy nodal electronic interactions in hole-doped cuprate superconductors, Nat. Commun. **10**, 5737 (2019).
[23] S. Smit, E. Mauri, L. Bawden, F. Heringa, F. Gerritsen, E. van Heumen, Y. K. Huang, T. Kondo, T. Takeuchi, N. E. Hussey, M. Allan, T. K. Kim, C. Cacho, A. Krikun, K. Schalm, H. T. C. Stoof, and M. S. Golden, Momentum-dependent scaling exponents of nodal self-energies measured in strange metal cuprates and modelled using semi-holography, Nat. Commun. **15**, 4581 (2024).
[24] J. M. Luttinger, Fermi surface and some simple equilibrium properties of a system of interacting fermions, Phys. Rev. **119**, 1153 (1960).
[25] S. Sachdev, *Quantum Phases of Matter* (Cambridge University Press, Cambridge, UK, 2023).
[26] C. M. Varma, P. B. Littlewood, S. Schmitt-Rink, E. Abrahams, and A. E. Ruckenstein, Phenomenology of the normal state of Cu-O high-temperature superconductors, Phys. Rev. Lett. **63**, 1996 (1989).
[27] C. M. Varma, *Colloquium:* Linear in temperature resistivity and associated mysteries including high temperature superconductivity, Rev. Mod. Phys. **92**, 031001 (2020).
[28] J. A. Hertz, Quantum critical phenomena, Phys. Rev. B **14**, 1165 (1976).
[29] S. Sachdev, *Quantum Phase Transitions* (Cambridge University Press, Cambridge, UK, 2011).
[30] T. Faulkner, H. Liu, J. McGreevy, and D. Vegh, Emergent quantum criticality, Fermi surfaces, and AdS_2, Phys. Rev. D **83**, 125002 (2011).
[31] Suppose that $v_F^\star > v$ and require that the pole remain outside the region of analyticity up to $\omega_2 = \Lambda$. This is not possible for a MFL. For a Hertz liquid with $\alpha < 1$ we obtain the constraint $v_F^\star/v < 1 + \lambda$. Thus here $v_F^\star$ can be greater than v, but not too much so.
[32] The coupling $\bar{\lambda}$ was defined via $\mathrm{Im}\,\bar{\Sigma} = -\bar{\lambda}|\omega|^\alpha/\omega_N^{\alpha-1}$, with ω_N a fiducial energy scale and $\bar{\Sigma} = \Sigma/\mathcal{A}$. Comparing to (13) we have $\mathcal{A}\bar{\lambda} = -|\lambda|(\frac{\omega_N}{\Lambda})^{\alpha-1}\cos\frac{\pi\alpha}{2}$. The nonuniversal quantity $\mathcal{A}$ is sensitive to physics outside the low-energy model and furthermore cannot be extracted from the published data analysis.
[33] S. D. Chowdhury, S. A. Hartnoll, A. Hebbar, and R. Khondaker, Bootstrapping transport in the Drude-Kadanoff-Martin model, arXiv:2509.18255.
[34] M. F. Paulos, J. Penedones, J. Toledo, B. C. van Rees, and P. Vieira, The S-matrix bootstrap. Part I: QFT in AdS, J. High Energy Phys. 11 (2017) 133.
[35] M. F. Paulos, J. Penedones, J. Toledo, B. C. van Rees, and P. Vieira, The S-matrix bootstrap II: Two dimensional amplitudes, J. High Energy Phys. 11 (2017) 143.
[36] M. F. Paulos, J. Penedones, J. Toledo, B. C. van Rees, and P. Vieira, The S-matrix bootstrap. Part III: Higher dimensional amplitudes, J. High Energy Phys. 12 (2019) 040.
[37] R. Rattazzi, V. S. Rychkov, E. Tonni, and A. Vichi, Bounding scalar operator dimensions in 4D CFT, J. High Energy Phys. 12 (2008) 031.
[38] S. El-Showk, M. F. Paulos, D. Poland, S. Rychkov, D. Simmons-Duffin, and A. Vichi, Solving the 3D Ising model with the conformal bootstrap, Phys. Rev. D **86**, 025022 (2012).
[39] D. Poland, S. Rychkov, and A. Vichi, The conformal bootstrap: Theory, numerical techniques, and applications, Rev. Mod. Phys. **91**, 015002 (2019).
[40] X. Han and S. A. Hartnoll, Locality bound for dissipative quantum transport, Phys. Rev. Lett. **121**, 170601 (2018).
[41] N. P. Armitage, Electrodynamics of correlated electron systems, arXiv:0908.1126.